IOP Publishing | Institute of Physics and Engineering in Medicine Physics in Medicine & Biology

Phys. Med. Biol. **61** (2016) 12–22 doi:10.1088/0031-9155/61/1/12

Assessing the radiation-induced second cancer risk in proton therapy for pediatric brain tumors: the impact of employing a patient-specific aperture in pencil beam scanning

Changran Geng[1,3], Maryam Moteabbed[1,2], Yunhe Xie[1], Jan Schuemann[1,2], Torunn Yock[1,2] and Harald Paganetti[1,2]

[1] Department of Radiation Oncology, Massachusetts General Hospital, Boston, MA 02114, USA
[2] Department of Radiation Oncology, Harvard Medical School, Boston, MA 02115, USA
[3] Department of Nuclear Science and Engineering, Nanjing University of Aeronautics and Astronautics, Nanjing 210016, People's Republic of China

E-mail: HPAGANETTI@mgh.harvard.edu

Received 21 July 2015, revised 25 October 2015
Accepted for publication 2 November 2015
Published 25 November 2015

Abstract

The purpose of this study was to compare the radiation-induced second cancer risks for in-field and out-of-field organs and tissues for pencil beam scanning (PBS) and passive scattering proton therapy (PPT) and assess the impact of adding patient-specific apertures to sharpen the penumbra in pencil beam scanning for pediatric brain tumor patients. Five proton therapy plans were created for each of three pediatric patients using PPT as well as PBS with two spot sizes (average sigma of ~17 mm and ~8 mm at isocenter) and choice of patient-specific apertures. The lifetime attributable second malignancy risks for both in-field and out-of-field tissues and organs were compared among five delivery techniques. The risk for in-field tissues was calculated using the organ equivalent dose, which is determined by the dose volume histogram. For out-of-field organs, the organ-specific dose equivalent from secondary neutrons was calculated using Monte Carlo and anthropomorphic pediatric phantoms. We find that either for small spot size PBS or for large spot size PBS, a patient-specific aperture reduces the in-field cancer risk to values lower than that for PPT. The reduction for large spot sizes (on average 43%)

is larger than for small spot sizes (on average 21%). For out-of-field organs, the risk varies only marginally by employing a patient-specific aperture (on average from −2% to 16% with increasing distance from the tumor), but is still one to two orders of magnitude lower than that for PPT. In conclusion, when pencil beam spot sizes are large, the addition of apertures to sharpen the penumbra decreases the in-field radiation-induced secondary cancer risk. There is a slight increase in out-of-field cancer risk as a result of neutron scatter from the aperture, but this risk is by far outweighed by the in-field risk benefit from using an aperture with a large PBS spot size. In general, the risk for developing a second malignancy in out-of-field organs for PBS remains much lower compared to PPT even if apertures are being applied.

Keywords: radiation-induced second cancer risk, proton therapy, TOPAS, aperture

(Some figures may appear in colour only in the online journal)

1. Introduction

Proton therapy (PT) is capable of decreasing the dose to organs at risk compared to photon therapy due to the physical character of the finite range. While intensity-modulated photon therapy (IMRT) can deliver comparable dose conformality to proton radiotherapy, the total energy deposited in the patient for any treatment will always be higher with photons than with protons (Paganetti 2011). Current proton therapy techniques are comprised of two main types: passive scattering proton therapy (PPT) and pencil beam scanning proton therapy (PBS). Compared to PPT, PBS reduces the dose to organs upstream of the target and reduces the neutron dose in the patient caused by scattering devices and apertures (Jiang *et al* 2005, Brenner and Hall 2008, Paganetti 2011). However, when the spot size in PBS is relatively large, the increased penumbral width can result in plans that are less favorable than PPT. The use of apertures in PBS can improve the penumbra. However, the use of apertures with PBS will increase the neutron dose to the patient.

Pediatric patients, who are more radiosensitive and have longer life expectancy, are especially susceptible to developing radiation-induced second cancers after radiation therapy (e.g. Li *et al* 1975, Nguyen *et al* 2008, Tukenova *et al* 2011). The risk for developing second malignancies from proton therapy has been studied extensively using various risk models. For example, Paganetti *et al* and Moteabbed *et al* studied the in-field second cancer risk comparing proton and photon therapy, and showed the overall advantage of proton therapy in terms of the second cancer risk for tissues close to the primary tumor site (Paganetti *et al* 2012, Moteabbed *et al* 2014). Further, out-of-field organs are exposed to scattered and secondary radiation, such as neutrons in proton therapy, associated with a cancer risk (see e.g. Brenner and Hall 2008, Zacharatou Jarlskog and Paganetti 2008, Xu *et al* 2008, Athar and Paganetti 2011).

Moteabbed *et al* assessed the improvements in plan quality when using apertures in PBS considering several pediatric patients with brain tumors (Moteabbed *et al* 2015). The independent goal of the work presented in this manuscript was to compare the radiation-induced second cancer risks for in-field and out-of-field organs and tissues for PBS and PPT and assess the impact of adding patient-specific apertures to sharpen the penumbra in PBS.

2. Materials and method

2.1. Treatment planning

Three pediatric patients, with astrocytoma, astrocytoma and ependymoma at age 14, 4 and 4 respectively, treated with PPT at Massachusetts General Hospital (MGH), were included in this study. For each patient, treatment plans were created and optimized using XIO (CMS Inc., St. Louis, Missouri) for PPT, and ASTROID (MGH in-house developed) for PBS. For the reference dose distributions in water XiO (PPT) and Astroid (PBS) have been validated with the Monte Carlo code TOAPS (Perl *et al* 2012) (see (Testa *et al* 2013) and (Grassberger *et al* 2015), respectively). The prescribed doses were 52.2 Gy(RBE) for patient 1 and 2, and 54 Gy(RBE) for patient 3. Five plans for each of the three cases were created and optimized using the following techniques: PPT, PBS with a large spot size (L-PBS), PBS with a large spot size using a patient-specific aperture (L-PBS-APT), PBS with a small spot size (S-PBS), PBS with a small spot size using a patient-specific aperture (S-PBS-APT). The large spot size refers to the energy dependent average sigma at isocenter of ~17 mm at 7 cm range, while for small spot size the average sigma at isocenter was assumed to be ~8 mm. The apertures were designed by the PPT planning system according to the shape and size of the clinical target volume (CTV) with an 8–10 mm aperture margin. Since PBS and PPT plans had the same beam direction and setup, the beam-specific apertures were identical for the two modalities.

2.2. Radiation-induced cancer risk estimation

For in-field tissues, the organ equivalent dose (OED) was calculated which considers inhomogeneous organ dose distributions and therapeutic dose levels (Schneider *et al* 2011). The OED was calculated on the basis of the Dose Volume Histogram (DVH) from the treatment plan following equation (1) (Schneider and Kaser-Hotz 2005).

$$\mathrm{OED} = \frac{1}{V}\sum_i V_i \frac{\mathrm{e}^{-\alpha_i' D_i}}{\alpha_i' R}\left(1 - 2R + R^2\mathrm{e}^{\alpha_i' D_i} - (1-R)^2\mathrm{e}^{-\frac{\alpha_i' R}{1-R}D_i} - \delta(-\alpha_i' R D_i)\right) \tag{1}$$

Here, i denotes the DVH bin number, V stands for the total organ volume, and V_i and D_i (in Gy(RBE)) are volume and dose in each bin. The model parameter δ is assumed to be 0 for carcinoma and 1 for sarcoma. Other parameters are the repopulation factor, R, and $\alpha^{'}$, the cell kill parameter obtained from the linear quadratic model (α and β) according to equation (2).

$$\alpha' = \alpha + \beta \mathrm{D}_i \frac{d_\mathrm{F}}{D} \tag{2}$$

The parameters for the OED calculations were taken from the literature (Preston *et al* 2007, Schneider *et al* 2011) and were previously used for in-field risk estimations (Moteabbed *et al* 2014). Note that because of the interplay between mutation and cell kill, the model results in a bell-shaped dose response curve for most organs/tissues. The OED for carcinoma and sarcoma induction was used to approximate the risk for a radiation-induced brain tumor. As a conservative alternative we also considered a purely linear dose response relationship.

For the out-of-field organs, the organ-specific dose equivalent (H_T) was determined using the mean organ dose and a radiation quality factor (ICRP 2003). The quality factor is better suited compared to the radiation weighting factor for in-patient doses (Xu and Paganetti 2010). The H_T was calculated using the linear energy transfer (LET) based quality factor $Q(\mathrm{LET})$ considering the mixed radiation field (equation (3)) (ICRP 2003).

$$H_{\mathrm{T}} = \frac{1}{m_{\mathrm{T}}} \int_{m_{\mathrm{T}}} \int_{\mathrm{LET}=0}^{\mathrm{LET}=\infty} Q(\mathrm{LET}) D_{\mathrm{LET}} \mathrm{dLET} \mathrm{d}m \tag{3}$$

Here, D_{LET} represents the distribution of absorbed dose considering the unrestricted LET and m_{T} stands for the mass of the organ T.

Risk models were applied to bridge the gap between dose and cancer induction risk. To estimate the second cancer risk, models are mostly based on the atomic bomb survivor data (BEIR 2006). In this study, two models, i.e. the excess relative risk (ERR) model and the excess absolute risk (EAR) model, were used to estimate the lifetime attributable risk (LAR) for a radiation-induced second cancer (equation (4)).

$$\mathrm{LAR} = \sum_{a=e+L}^{a=75} \left(\mathrm{e}^{(log(\mathrm{ERR}\times\lambda)\times\eta)+log(\mathrm{EAR})\times(1-\eta)} \times \frac{S(a)}{S(e)} \right) \times H \Big/ \mathrm{DDREF} \tag{4}$$

Here, e is the age at exposure, L is the latent time after the exposure, H is the equivalent dose (defined as OED for in-field tissues and H_{T} for out-of-field organs), η is used to weight the ERR and EAR models, and $S(a)/S(e)$ is the probability of surviving from age e to a (Howlader *et al* 2015). We assumed the dose and dose-rate reduction effect (DDREF) as unity for the high-LET radiation (ICRP 2003, BEIR 2006). Parameter values and detail information with respect to EAR and ERR for out-of-filed risk calculations can be found in the BEIR report (BEIR 2006). For in-field tissues, only the EAR model and parameters were considered following the recommendation previously published (Schneider *et al* 2008, Schneider *et al* 2011).

2.3. The Monte Carlo method and anthropomorphic phantoms

The dose distributions (in Gy(RBE)) for in-field tissues were extracted from the treatment planning systems. Dose calculations (in Gy and then weighted by the quality factor) for out-of-field organs were performed using Monte Carlo, i.e. TOPAS (Perl *et al* 2012). The LET, which was used for quality factor evaluation in equation (3), was calculated by dividing the deposited energy by the step length of the interaction step for charged particles (see (Grassberger and Paganetti 2011) for details). To calculate the out-of-field organ doses, 4 and a 14 year-old whole body anthropomorphic computational phantoms from the UF-hybrid phantom series (Lee *et al* 2005) were implemented in the Monte Carlo environment to replace the 4 year-old and 14 year-old patient geometry, respectively. For illustration, the simulation of the 14 year-old patient treated by L-PBS-APT is shown in figure 1.

3. Results and discussion

3.1. Lifetime attributable risk: in-field

As tissue contour to represent the in-field soft tissues we used the brain excluding the CTV. Figure 2 shows dose volume histograms for the in-field soft tissues for the five techniques and the three patients. Figure 3 shows LARs for brain tumor induction calculated by the Schneider risk models and the linear dose-response model. As expected, the linear model results in greater LAR for all techniques compared to the full dose-response models. It has previously been shown that the LAR for skull is always lower than that for soft-tissues in the brain (Moteabbed *et al* 2014). Thus, we only considered LAR for soft-tissue as a conservative end point.

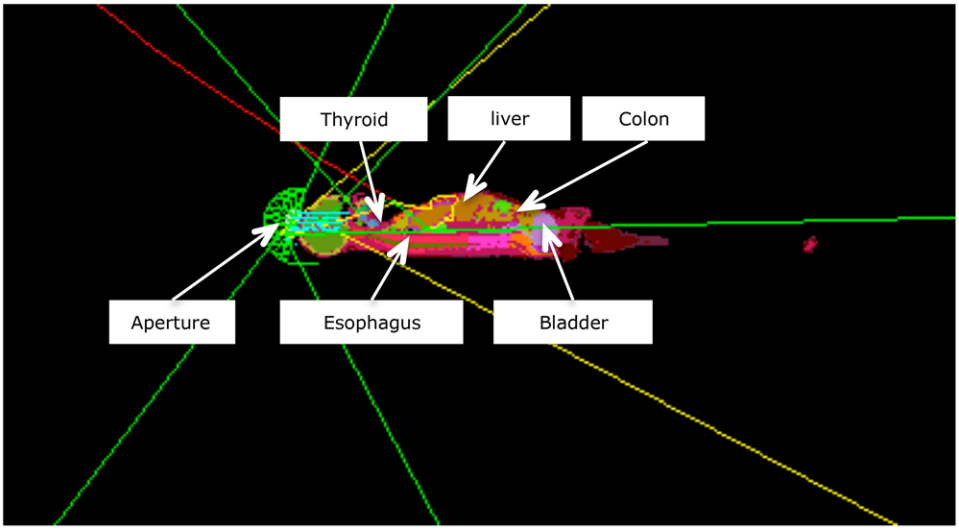

Figure 1. Illustration of a 14 year-old whole body phantom irradiated by pencil beam scanning proton therapy with a large spot size and patient-specific aperture in TOPAS. Trajectories for different particle are plotted by different color, i.e. cyan (proton), yellow (neutron), green (gamma), red (electron).

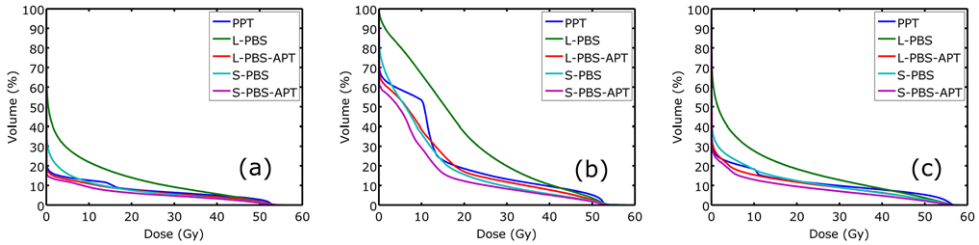

Figure 2. Dose–volume histograms for in-field soft tissue, as represented by the whole brain excluding the CTV volume, for five treatment plans for three patients. (a) Patient 1: 14 year-old male; prescribed dose of 52.2 Gy (RBE); (b) patient 2: 4 year-old female; prescribed dose of 52.2 Gy (RBE); (c) patient 3; 4 year-old female; prescribed dose of 54 Gy (RBE).

As expected from the DVHs (figure 2), the in-field risk for L-PBS is considerably larger than for S-PBS due to the larger penumbra. Adding an aperture reduces the penumbra and thus the in-field risk (e.g. as in S-PBS-APT). For instance, as shown in figure 4, the risks decreases on average by 43% for the large spot size and by 21% for the small spot size using the linear model. A similar trend can be found for the non-linear model.

Note that the LARs of in-field tumor for PPT are smaller than that for L-PBS due to the considered large spot sizes in L-PBS which does not offer a dose conformality advantage compared to PPT. The LARs for PPT are larger than for L-PBS-APT, S-PBS, and S-PBS-APT.

3.2. Lifetime attributable risk: out-of-field

We have demonstrated above that using an aperture reduces the in-field dose and thus risk significantly. This gain has to be balanced against the risk caused by secondary radiation generated by an aperture.

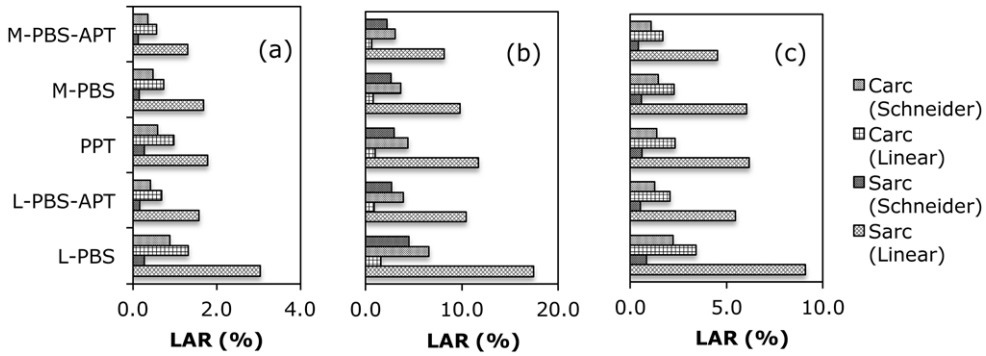

Figure 3. LAR in % for second tumor induction of in-field soft tissues calculated using Schneider risk models and the linear dose-response model. (a) Patient 1: 14 year-old male; prescribed dose of 52.2 Gy (RBE); (b) patient 2: 4 year-old female; prescribed dose of 52.2 Gy (RBE); (c) patient 3: 4 year-old female; prescribed dose of 54 Gy (RBE).

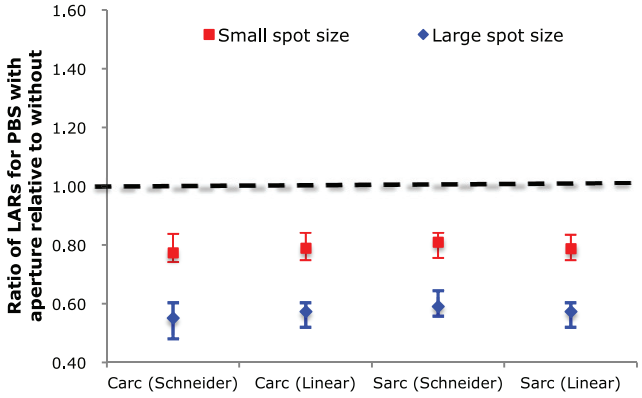

Figure 4. Ratios of LARs for PBS with aperture relative to that of PBS without aperture for in-field tumors. The upper and lower error bars represent the maximum and minimum values among the three cases considered.

Figure 5 shows the neutron dose equivalents for out-of-field organs for the considered five proton delivery techniques. The dose equivalent for leukemia was determined by the average dose absorbed in all skeletal components that were not irradiated by the primary beam. As expected, neutron dose equivalents for PPT show the highest values for all cases due to the secondary neutrons generated in the treatment head. The figure also shows a decreasing trend with increasing distance to the target.

Apparently, the dose differences between PBS with and without apertures are insignificant for all organs because the aperture was solely used to cut the penumbra instead of blocking a large beam as in PPT. For the first and second patients, the addition of apertures can even slightly reduce the neutron dose equivalent for organs such as the esophagus and thyroid, which are relatively close to the target (see figure 5). This is because instead of generating neutrons due to protons stopping in the patient, they are now produced by stopping protons in the upstream aperture. Depending on the patient geometry, this can reduce the neutron dose. For the third patient, the patient-specific aperture increases the neutron dose equivalent for all organs, but the dose is still far below that from PPT.

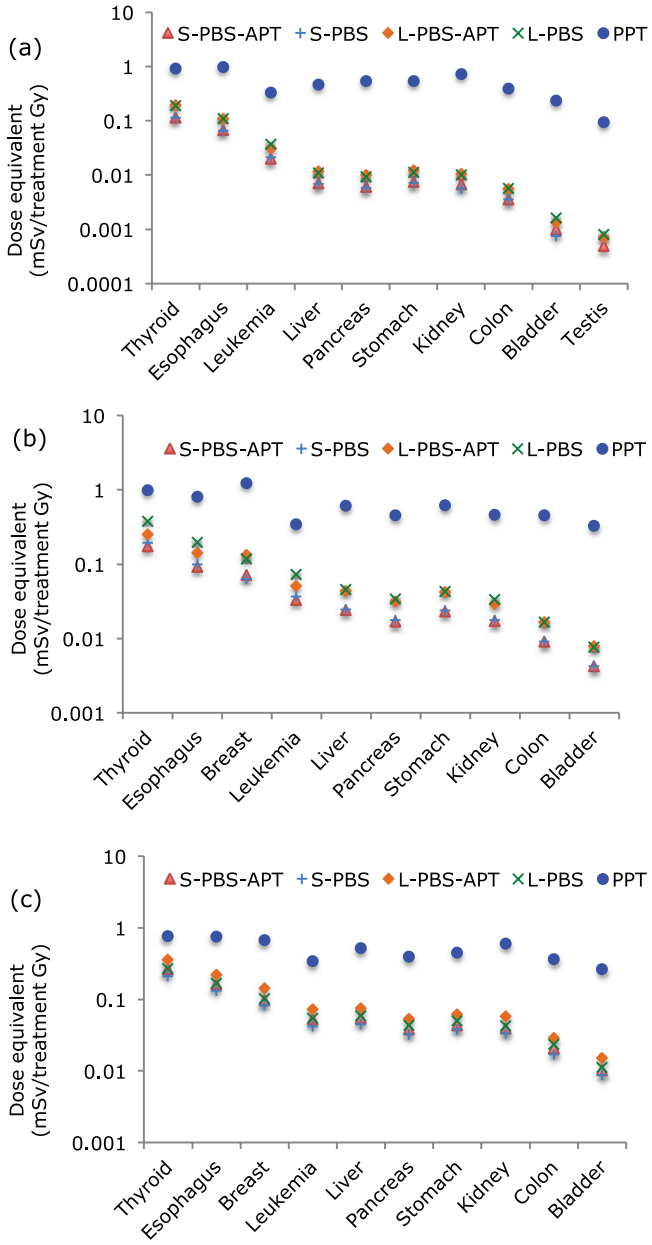

Figure 5. Neutron dose equivalent for out of field organs. (a) Patient 1: 14 year-old male; (b) patient 2: 4 year-old female; (c) patient 3: 4 year-old female.

Table 1 lists the LAR values for the out-of-field organs for the three cases. The risks for the 4 year-old females are higher than the 14 year-old male, which is attributed to not only the shorter body length and thus shorter distance from target to normal organs, but also the longer life expectancy.

Figure 6 illustrates the average ratios of LARs for PBS with aperture relative to that of PBS without aperture for the out-of-field organs. The upper and lower bars show the maximum

Table 1. Lifetime attributable risk (%) for second cancer incidences for out-of-field organs for a course of proton therapy.

Organs	S-PBS		S-PBS-APT		L-PBS		L-PBS-APT		PPT	
Age (gender)[a]	14 (M)	4 (F)	14 (M)	4 (F)	14 (M)	4 (F)	14 (M)	4 (F)	14 (M)	4 (F)
Pancreas	0.0002	0.0016	0.0002	0.0017	0.0003	0.0024	0.0004	0.0027	0.0197	0.0261
Kidney	0.0003	0.0021	0.0004	0.0024	0.0006	0.0032	0.0006	0.0037	0.0428	0.0436
Esophagus	0.0017	0.0021	0.0017	0.0023	0.0029	0.0033	0.0029	0.0033	0.0256	0.0140
Bladder	0.0000	0.0005	0.0001	0.0006	0.0001	0.0008	0.0001	0.0009	0.0142	0.0230
Leukemia[b]	0.0011	0.0024	0.0010	0.0027	0.0019	0.0039	0.0016	0.0038	0.0176	0.0214
Liver	0.0002	0.0006	0.0002	0.0007	0.0003	0.0009	0.0004	0.0010	0.0139	0.0093
Colon	0.0004	0.0012	0.0004	0.0014	0.0006	0.0018	0.0006	0.0021	0.0424	0.0365
Stomach	0.0002	0.0014	0.0002	0.0015	0.0003	0.0020	0.0003	0.0023	0.0128	0.0227
Testes/breast[c]	0.0000	0.0405	0.0000	0.0464	0.0000	0.0606	0.0000	0.0762	0.0042	0.5190
Thyroid	0.0049	0.1245	0.0049	0.1350	0.0082	0.1980	0.0083	0.1890	0.0396	0.5405

[a] Values for 4(F) were averaged over the second and the third patient.
[b] The leukemia risk estimation was determined by averaging the dose among all skeletal components that were not irradiated by the primary beam.
[c] Testes for 14 year-old male; breast for 4 year-old female.

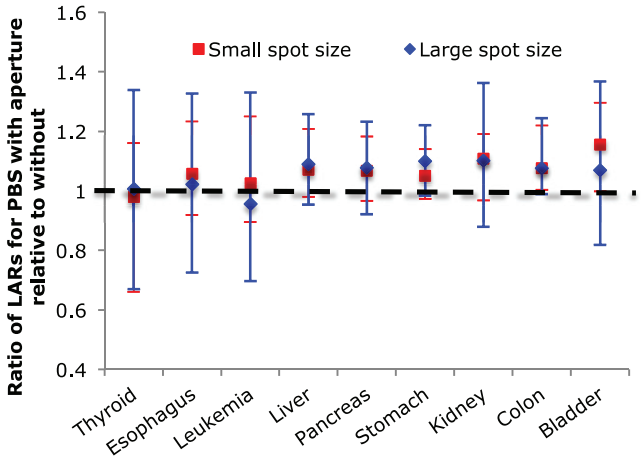

Figure 6. Ratios of LARs for PBS with aperture relative to that of PBS without aperture for out-of-field organs. The upper and lower bar shows the maximum and minimum value among the three cases.

and minimum values among the three cases. This shows that the risk increased on average by ~10% when adding an aperture in PBS. The maximum increase is 45% for thyroid for patient 3. We also find an increase of the ratio, on average from 0.98 (thyroid) to 1.16 (bladder) with increasing distance from the target considering both small and large spot size PBS. It had been shown previously that the out-of-field dose decreases near the target and increases at ~50 cm away from the field edge when comparing the values for PBS with and without patient-specific apertures in a homogeneous phantom geometry (Dowdell *et al* 2012).

For the linear no-threshold model used for LAR for out-of-field organs, the organ lifetime attributable risk for PPT is about one to two orders of magnitude larger than that for PBS regardless of the use of apertures. Thus, the increase in risk stemming from the aperture is by far outweighed by the decrease in in-field risk.

There are considerable uncertainties associated with cancer risk models and model parameters, e.g. the quality factor and the dose and dose rate effect (Schneider and Kaser-Hotz 2005). However, our study focuses on the comparison of different proton treatment modalities on the radiation induced second cancer, thus the uncertainties cancel out to some extent (Kry *et al* 2007, Nguyen *et al* 2015).

4. Conclusions

In summary, this study compared the radiation-induced second cancer risks for in-field and out-of-field organs and tissues for PBS and PPT, and assessed the second tumor induction risk from the use of apertures in scanning beam techniques. The results show that the radiation-induced second cancer risks for in-field tumors for L-PBS are higher than that for PPT due to the degraded (enlarger) penumbra. With apertures in PBS the penumbra is sharpened which results in a decrease in second cancer risk due to an overall decrease of integral dose. The LAR values of out-of-field organs from PBS are significantly lower than that of PPT regardless of whether or not patient-specific apertures are used. We found on average a small increase in the LAR for out of field organs due to neutrons generated in the aperture for PBS with aperture. However, these were outweighed by the overall sparing advantage in-field and in the penumbral region.

Acknowledgment

One of the authors (CG) was funded by the China Scholarship Council (CSC) and the National Natural Science Foundation of China (Grant No. 11475087). We would like to thank the MGH Monte Carlo group for many fruitful discussions and the Partners Research Computing group for maintaining the computer cluster.

References

Athar B S and Paganetti H 2011 Comparison of second cancer risk due to out-of-field doses from 6 MV IMRT and proton therapy based on 6 pediatric patient treatment plans *Radiother. Oncol.* **98** 87–92

BEIR 2006 *Health Risks from Exposure to Low Levels of Ionizing Radiation BIER VII Phase 2* (Washington, DC: National Research Council, Academy of Science)

Brenner D J and Hall E J 2008 Secondary neutrons in clinical proton radiotherapy: a charged issue *Radiother. Oncol.* **86** 165–70

Dowdell S J, Clasie B, Depauw N, Metcalfe P, Rosenfeld A B, Kooy H M, Flanz J B and Paganetti H 2012 Monte Carlo study of the potential reduction in out-of-field dose using a patient-specific aperture in pencil beam scanning proton therapy *Phys. Med. Biol.* **57** 2829–42

Grassberger C, Lomax A and Paganetti H 2015 Characterizing a proton beam scanning system for Monte Carlo dose calculation in patients *Phys. Med. Biol.* **60** 633–45

Grassberger C and Paganetti H 2011 Elevated LET components in clinical proton beams *Phys. Med. Biol.* **56** 6677–91

Howlader N *et al* 2015 *Cancer Statistics Review, 1975–2012* (Bethesda, MD: National Cancer Institute)

ICRP 2003 *Relative Biological Effectiveness, Radiation Weighting and Quality Factor ICRP Publication 92* (Oxford: Pergamon)

Jiang H, Wang B, Xu X G, Suit H D and Paganetti H 2005 Simulation of organ-specific patient effective dose due to secondary neutrons in proton radiation treatment *Phys. Med. Biol.* **50** 4337–53

Kry S F, Followill D, White R A, Stovall M, Kuban D A and Salehpour M 2007 Uncertainty of calculated risk estimates for secondary malignancies after radiotherapy *Int. J. Radiat. Oncol. Biol. Phys.* **68** 1265–71

Lee C, Williams J L, Lee C and Bolch W E 2005 The UF series of tomographic computational phantoms of pediatric patients *Med. Phys.* **32** 3537–48

Li F P, Cassady J R and Jaffe N 1975 Risk of second tumors in survivors of childhood cancer *Cancer* **35** 1230–5

Moteabbed M, Yock T I, Depauw N, Kooy H M and Paganetti H 2015 When does pencil beam scanning become superior to passive scattered proton therapy for pediatric head and neck cancers? *Int. J. Radiat. Oncol. Biol. Phys.* submitted

Moteabbed M, Yock T I and Paganetti H 2014 The risk of radiation-induced second cancers in the high to medium dose region: a comparison between passive and scanned proton therapy, IMRT and VMAT for pediatric patients with brain tumors *Phys. Med. Biol.* **59** 2883–99

Nguyen J, Moteabbed M and Paganetti H 2015 Assessment of uncertainties in radiation-induced cancer risk predictions at clinically relevant doses *Med. Phys.* **42** 81–9

Nguyen F, Rubino C, Guerin S, Diallo I, Samand A, Hawkins M, Oberlin O, Lefkopoulos D and De Vathaire F 2008 Risk of a second malignant neoplasm after cancer in childhood treated with radiotherapy: correlation with the integral dose restricted to the irradiated fields *Int. J. Radiat. Oncol. Biol. Phys.* **70** 908–15

Paganetti H 2011 *Proton Therapy Physics* (Boca Raton, FL: CRC)

Paganetti H, Athar B S, Moteabbed M, Adams J A, Schneider U and Yock T I 2012 Assessment of radiation-induced second cancer risks in proton therapy and IMRT for organs inside the primary radiation field *Phys. Med. Biol.* **57** 6047–61

Perl J, Shin J, Schümann J, Faddegon B and Paganetti H 2012 TOPAS: an innovative proton Monte Carlo platform for research and clinical applications *Med. Phys.* **39** 6818

Preston D L, Ron E, Tokuoka S, Funamoto S, Nishi N, Soda M, Mabuchi K and Kodama K 2007 Solid cancer incidence in atomic bomb survivors: 1958–1998 *Radiat. Res.* **168** 1–64

Schneider U and Kaser-Hotz B 2005 Radiation risk estimates after radiotherapy: application of the organ equivalent dose concept to plateau dose-response relationships *Radiat. Environ. Biophys.* **44** 235–9

Schneider U, Lomax A and Timmermann B 2008 Second cancers in children treated with modern radiotherapy techniques *Radiother. Oncol.* **89** 135–40

Schneider U, Sumila M and Robotka J 2011 Site-specific dose-response relationships for cancer induction from the combined Japanese A-bomb and Hodgkin cohorts for doses relevant to radiotherapy *Theor. Biol. Med. Modelling* **8** 27

Testa M, Schumann J, Lu H M, Shin J, Faddegon B, Perl J and Paganetti H 2013 Experimental validation of the TOPAS Monte Carlo system for passive scattering proton therapy *Med. Phys.* **40** 121719

Tukenova M *et al* 2011 Radiation therapy and late mortality from second sarcoma, carcinoma, and hematological malignancies after a solid cancer in childhood *Int. J. Radiat. Oncol. Boil. Phys.* **80** 339–46

Xu X G, Bednarz B and Paganetti H 2008 A review of dosimetry studies on external-beam radiation treatment with respect to second cancer induction *Phys. Med. Biol.* **53** R193–241

Xu X G and Paganetti H 2010 Better radiation weighting factors for neutrons generated from proton treatment are needed *Radiat. Prot. Dosim.* **138** 291–4

Zacharatou Jarlskog C and Paganetti H 2008 Risk of developing second cancer from neutron dose in proton therapy as function of field characteristics, organ, and patient age *Int. J. Radiat. Oncol. Biol. Phys.* **72** 228–35